

Constraints on Dark Matter-Photon Coupling in the Presence of Time-Varying Dark Energy

Santosh Kumar Yadav¹

Department of Mathematics, BITS Pilani, Pilani Campus, Rajasthan-333031, India.

Abstract: In a recent work [Phys. Rev. D 98, 043521 (2018)], we have investigated a dark matter (DM)-photon coupling model in which the DM decays into photons in the presence of dark energy (DE) with constant equation of state (EoS) parameter. Here, we study an extension of the DM-photon coupling model by considering a time-varying EoS of DE via Chevalier-Polarski-Linder (CPL) parametrization. We derive observational constraints on the model parameters by using the data from cosmic microwave background (CMB), baryonic acoustic oscillations (BAO), the local value of Hubble constant from Hubble Space Telescope (HST), and large scale structure (LSS) information from the abundance of galaxy clusters, in four different combinations. We find that in the present DM-photon coupling scenario the mean values of $w_{\text{de}0}$ are in quintessence region ($w_{\text{de}0} > -1$) whereas they were in the phantom region ($w_{\text{de}0} < -1$) in our previous study with all data combinations. The constraints on the DM-photon coupling parameter do not reflect any significant deviation from the previous results. Due to the decay of DM into photons, we obtain higher values of H_0 , consistent with the local measurements, similar to our previous study. But, the time-varying DE leads to lower values of σ_8 in the DM-photon coupling model with all data combinations, in comparison to the results in our previous study. Thus, allowing time-varying DE in the DM-photon coupling scenario is useful to alleviate the H_0 and σ_8 tensions.

PACS: 95.35.+d, 95.36.+x, 98.80.Cq

1 Introduction

The major matter component, namely, dark matter (DM) is a mysterious component of the Universe whose precise nature is still an open question in modern cosmology. In the literature, many attempts have been made via direct and indirect searches to know about the nature/properties of DM like mass, spin, parity, interaction cross-section etc. but very less is known concretely so far. See [1, 2] for a review about the evidences, candidates and methods of detection of DM. The phenomenon of decay of DM into species like dark radiation, photons, neutrinos etc. has been considered in the literature in different contexts and motivations. A review of decaying DM signals in gamma-rays, cosmic ray antimatter and neutrinos can be seen in [3]. More intensively, the search for DM decay has been carried out using the IceCube telescope data [4]. Many theoretical/phenomenological studies have been carried out with DM decay models in order to look for some possible solutions to the problems associated with the standard Λ CDM cosmology. For instance, the evidence for DM-dark radiation interaction is reported in [5] where it has been found that this interaction allows to reconcile the σ_8 tension between Planck cosmic microwave background (CMB) and large scale structure (LSS) measurements. It has been observed in [6, 7] that the late-time decay of DM is helpful in reconciling some of the small-scale structure formation problems associated with the standard Λ CDM cosmology. Also see [8, 9, 10, 11, 12, 13, 14], where the interaction between DM and dark radiation has been investigated.

The decay of DM into photons (and photons + neutrinos) has been investigated from cosmic-ray emission in [15, 16, 17]. An analytical and numerical study of DM-photon interactions have been performed in [18] where some consequences of DM-photon interaction on structure formation have been explored. Recently, the constraints on DM-photon scattering-cross section in the early Universe have been obtained in [19]. The upper bounds on the decay width of DM into different final states can be investigated by searching decaying DM. An upper limit on the DM-photon elastic scattering cross section $\sigma_{\text{DM}-\gamma} \lesssim 10^{-32} (m_{\text{DM}}/\text{GeV}) \text{ cm}^2$ has been derived in [20]. An upper bound on elastic scattering cross section of DM-neutrino and DM-dark energy (DE) have been obtained as $\sigma_{\text{DM}-\nu} \lesssim 10^{-33} (m_{\text{DM}}/\text{GeV}) \text{ cm}^2$ and $\sigma_{\text{DM}-\text{DE}} \lesssim 10^{-29} (m_{\text{DM}}/\text{GeV}) \text{ cm}^2$ in [21] and [22], respectively.

Recently, we (two more authors) have studied a DM-photon coupling model in [23], where the constraints on decay rate of DM into photons, and possible consequences of the coupling scenario are investigated in the presence of DE with constant equation of state (EoS) parameter. In the work [23], we have considered interaction

¹E-mail: sky91bbaulko@gmail.com

between DM and photons where the DM decay into photons takes place throughout the cosmic history of the Universe, leading to non-conservation of the particle number densities for both the species. Note that this interaction is different from the DM-photon elastic scattering interaction considered in [19, 20, 21, 22], where the particle number density remains conserved. Here, we present a follow-up study of [23] by considering a time-varying EoS of DE via Chevalier-Polarski-Linder (CPL) parametrization [24, 25]. The main aim of this work is to investigate the possible changes/effects of time-varying DE on the results of the DM-photon coupling scenario obtained in our recent study [23]. We constrain this scenario by using recent data from CMB, baryonic acoustic oscillations (BAO), the local value of Hubble constant from Hubble Space Telescope (HST), and LSS information from the abundance of galaxy clusters, in four different combinations.

The rest of this work is organized as follows. In the next Section 2, we describe the DM-photon coupling model and discuss the possible effects of variable EoS of DE on CMB temperature (TT) and matter power spectra. Section 3 describes the observational data and methodology used in this work. In Section 4, we derive observational constraints and discuss the results. We conclude the main findings of this study in Section 6. In what follows, a subindex 0 attached to any quantity denotes its present value and a prime over a quantity represents its derivative with respect to conformal time.

2 DM-photon Coupling Model with Time-varying Dark Energy

In this section, we reproduce the DM-photon coupling scenario and the related perturbation equations considered in our recent study [23] while inducing the time-varying EoS of DE via CPL parametrization. We assume that, in the framework of Friedmann-Lemaître-Robertson-Walker (FLRW) Universe, DM decays into photons via the the following background density equations:

$$\rho'_{\text{ddm}} + 3\frac{a'}{a}\rho_{\text{ddm}} = -\frac{a'}{a}\Gamma_{\gamma}\rho_{\text{ddm}}, \quad (1)$$

$$\rho'_{\gamma} + 4\frac{a'}{a}\rho_{\gamma} = \frac{a'}{a}\Gamma_{\gamma}\rho_{\text{ddm}}, \quad (2)$$

where the dimensionless parameter Γ_{γ} characterizes the DM-photons coupling. The quantities ρ_{ddm} and ρ_{γ} denote energy density of decaying DM and photons, respectively.

For the i th coupled component, the covariant conservation equation allowing for energy-momentum transfer gives $\nabla_{\mu}T_i^{\nu\mu} = Q_i^{\nu}$. The requirement of the conservation of the total energy-momentum, $\nabla_{\mu}T^{\nu\mu} = 0$, demands $\sum_i Q_i^{\nu} = 0$. Here, it is satisfied with $Q_{\text{ddm}} = -\frac{a'}{a}\Gamma_{\gamma}\rho_{\text{ddm}}$ and $Q_{\gamma} = \frac{a'}{a}\Gamma_{\gamma}\rho_{\text{ddm}}$. Note that a non-conservation in the number density of DM particles results in non-conservation of the energy-momentum tensor of the DM particles. We assume $\Gamma_{\gamma} > 0$ to have a decaying DM throughout the expansion history of the Universe. In general, the DM decay rate is considered to be constant but it could also be time-varying as well. We define decay rate as follows: $\Gamma = \Gamma_{\gamma}\mathcal{H}/a$, where \mathcal{H} is conformal Hubble parameter. Here, we extend our previous analysis [23] by considering a time-varying EoS of DE via CPL parametrization [24, 25, 26, 27], given by

$$w_{\text{de}}(a) = w_{\text{de}0} + w_{\text{de}1}(1 - a), \quad (3)$$

where $w_{\text{de}0}$ and $w_{\text{de}1}$ are free parameters (constants) to be constrained by the observational data. The evolution of density of decaying DM and photons can be easily found from eqs. (1) and (2) or more explicitly see eqs. (3) and (4) in [23].

2.1 Perturbation Equations

In the present work, we consider the linear perturbations in synchronous gauge via the line element of the linearly perturbed FLRW metric:

$$ds^2 = -a^2 d\tau^2 + a^2[(1 - 2\eta)\delta_{ij} + 2\partial_i\partial_j E]dx^i dx^j, \quad (4)$$

where $k^2 E = -2/h - 3\eta$, restricted to the scalar modes h and η . Then, using $\nabla_{\mu}T_i^{\nu\mu} = Q_i^{\nu}$, the continuity and Euler equations of the i th coupled fluid read as follows:

$$\begin{aligned} \delta'_i + 3\mathcal{H}(c_{s,i}^2 - w_i)\delta_i + 9\mathcal{H}^2(1 + w_i)(c_{s,i}^2 - c_{a,i}^2)\frac{\theta_i}{k^2} + (1 + w_i)\theta_i - 3(1 + w_i)\eta' + (1 + w_i)\left(\frac{h'}{2} + 3\eta'\right) \\ = \frac{a}{\rho_i}(\delta Q_i - Q_i\delta_i) + a\frac{Q_i}{\rho_i}\left[3\mathcal{H}(c_{s,i}^2 - c_{a,i}^2)\right]\frac{\theta_i}{k^2}, \end{aligned} \quad (5)$$

$$\theta'_i + \mathcal{H}(1 - 3c_{s,i}^2)\theta_i - \frac{c_{s,i}^2}{(1 + w_i)}k^2\delta_i = \frac{aQ_i}{(1 + w_i)\rho_i}\left[\theta_{\text{ddm}} - (1 + c_{s,i}^2)\theta_i\right], \quad (6)$$

where $c_{a,i}^2$, $c_{s,i}^2$ and w_i , respectively represent the adiabatic sound speed, physical sound speed and EoS of the i th fluid in the rest frame (See [28] and references therein for such a methodology to describe the linear perturbations of the interaction between DM and DE).

Further, by particularizing the fluid approximation equations to the DM and photon coupled system, the continuity and Euler equations for photons, respectively, read as follows:

$$\delta'_\gamma + \frac{4}{3}\theta_\gamma + \frac{2}{3}h' = a\Gamma_\gamma\mathcal{H}\frac{\rho_{\text{ddm}}}{\rho_\gamma}(\delta_{\text{ddm}} - \delta_\gamma), \quad (7)$$

$$\theta'_\gamma - \frac{1}{4}k^2(\delta_\gamma - 4\sigma_\gamma) - an_e\sigma_T(\theta_b - \theta_\gamma) = \frac{3}{4}a\Gamma_\gamma\mathcal{H}\frac{\rho_{\text{ddm}}}{\rho_\gamma}(\theta_{\text{ddm}} - \frac{4}{3}\theta_\gamma), \quad (8)$$

where θ_b is the divergence of baryons fluid velocity, and $an_e\sigma_T(\theta_b - \theta_\gamma)$ appears due to the collision between photons and baryons before recombination. The momentum transfer is chosen in the rest frame of DM. The DM evolution is given by

$$\delta'_{\text{ddm}} + \frac{h'}{2} = 0. \quad (9)$$

In the synchronous gauge, the Euler equation for DM reads as

$$\theta_{\text{ddm}} = 0. \quad (10)$$

2.2 Effects on Matter and CMB TT Power Spectra

As discussed in our previous study [23], the matter power spectrum, CMB anisotropies, CMB spectral distortions, luminosity distance etc. can be affected in various ways due to the non-conservation of the photon number density resulting from the decay of DM into photons.

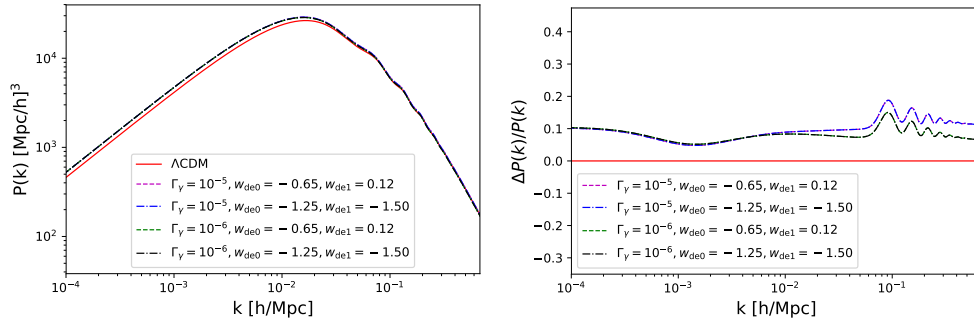


Figure 1: The matter power spectrum and its relative deviations from standard ΛCDM model for some values of Γ_γ , $w_{\text{de}0}$ and $w_{\text{de}1}$ mentioned in legend whereas the other related parameters are kept to their respective mean value from Table 2.

Figure 1 and Fig. 2 respectively show the matter and CMB TT power spectra with their relative deviations from standard ΛCDM model for some values of the parameters Γ_γ , $w_{\text{de}0}$ and $w_{\text{de}1}$, as mentioned in legends

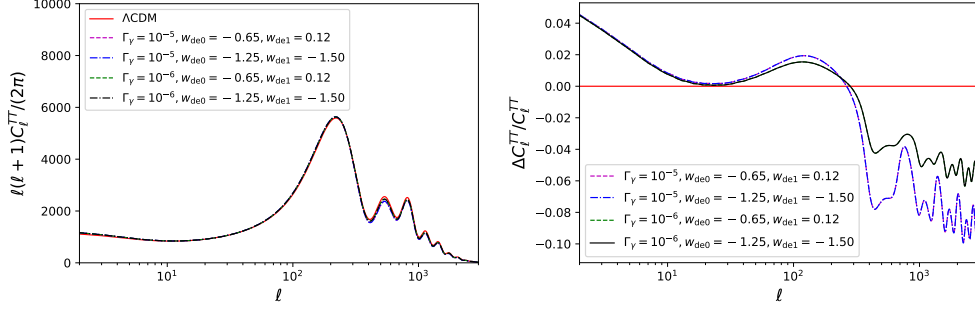


Figure 2: The CMB TT power spectrum and its relative deviations from standard Λ CDM model for some values of Γ_γ , w_{de0} and w_{de1} mentioned in legend whereas the other related parameters are kept to their respective mean value from Table 2.

whereas the other related parameters are kept to their respective mean value from Table 2. We notice that the two spectra deviate considerably from the Λ CDM model due to change in Γ_γ as we observed in our previous study. On the other hand, no deviations are observed due to change in the EoS parameters of DE. Thus, the time-varying DE does not affect the matter and CMB power spectra on the top of the DM-photon coupling scenario.

In any general modification of Λ CDM cosmology (within DE models), it is expected that the main effects of CMB anisotropies occur on the amplitude of the late time integrated Sachs-Wolfe (ISW) effect, manifested at large angular scales. This effect depends on the duration of the DE domination, i.e., on the time of equality of matter and DE density. So, different behaviors of $w(z)$ (in this case from CPL model), quintessence or phantom behavior must have opposite effects in $l < 100$. So, the values of w_{de0} and w_{de1} can be fixed in such a way that DE will show quintessence or phantom behavior at late time (for instance, for $z < 2$). The constraints on total matter density (Ω_m) control the amplitude of peaks, especially the second and third peaks. It can be seen from Table 2, that the changes on Ω_m are minimal, so the amplitude corrections will also be minimal. Also, changes in the expansion of the Universe, at late time from CPL free parameters and early times from Γ_γ will contribute to the corrections on the amplitude of all peaks and shifts on the spectrum due to the modification in the angular diameter distance at decoupling (depend on the expansion history of the DM-photon interaction model after decoupling). The magnitudes of corrections are proportional to the possible deviations from the values, $\Gamma_\gamma = 0$, $w_{de0} = -1$, and $w_{de1} = 0$, compared with minimal Λ CDM model. Note that in our work, $\Gamma_\gamma \ll 1$. The coupling parameter Γ_γ will contribute at small scales because it changes the density of photons at $z \gg 1$.

3 Data, Methodology and Model Parameters

The observational data sets used to derive constraints on various model parameters are described briefly as follows.

CMB: Planck cosmic microwave background data consisting of high- l (TT), low- l polarisation and Planck lensing survey from Planck-2015 [29].

BAO: Four baryon acoustic oscillations observations from the Six Degree Field Galaxy Survey (6dFGS) at $z_{\text{eff}} = 0.106$ [30], the Main Galaxy Sample of Data Release 7 of Sloan Digital Sky Survey (SDSS-MGS) at $z_{\text{eff}} = 0.15$ [31], the LOWZ and CMASS galaxy samples of Data Release 11 of the Baryon Oscillation Spectroscopic Survey (BOSS) LOWZ and BOSS-CMASS at $z_{\text{eff}} = 0.32$ and $z_{\text{eff}} = 0.57$, respectively [32]. These BAO observations are summarized in Table I of [33].

HST: The local value of Hubble constant, $H_0 = 73.24 \pm 1.74 \text{ km s}^{-1} \text{ Mpc}^{-1}$ by Hubble Space Telescope (HST) [34].

LSS: Three large scale structure (LSS) observations, including the measurements from the Sunyaev-Zeldovich

Table 1: Uniform priors on model parameters used in the present work.

Parameter	Prior
$100\omega_b$	[1.8, 2.4]
ω_{cdm}	[0.001, 0.99]
$100\theta_s$	[0.5, 10.0]
$\ln[10^{10}A_s]$	[2.7, 4.0]
n_s	[0.9, 1.1]
τ_{reio}	[0.01, 0.9]
w_{de0}	[-2.0, 0.5]
w_{de1}	[-1.5, 1.5]
$\sum m_\nu$	[0.06, 1.0]
N_{eff}	[1.0, 4.0]
Γ_γ	[0, 0.0001]

(SZ) effect cluster mass function: $\sigma_8 \left(\frac{\Omega_m}{0.27}\right)^{0.30} = 0.782 \pm 0.010$ [35]; weak gravitational lensing data from Canada-France-Hawaii Telescope Lensing Survey (CFHTLenS): $\sigma_8 \left(\frac{\Omega_m}{0.27}\right)^{0.46} = 0.774 \pm 0.040$ [36]; and the weak gravitational lensing shear power spectrum constraints: $\sigma_8 \left(\frac{\Omega_m}{0.30}\right)^{0.50} = 0.651 \pm 0.058$ from the Kilo Degree Survey (KiDS-450) [37].

The underlying model is implemented in publicly available CLASS [38] code, and the parameter inference is done by using the Monte Python [39] code which is embedded with Metropolis Hastings algorithm and interfaced with CLASS code to obtain correlated Markov Chain Monte Carlo (MCMC) samples. The uniform priors used in this work are mentioned in Table 1. The correlated MCMC samples are obtained with four different data combinations: CMB + BAO, CMB + BAO + HST, CMB + BAO + LSS, and CMB + BAO + HST + LSS. The convergence of the Monte Carlo Markov Chains is checked by Gelman-Rubin criteria [40] which requires $1 - R < 0.03$ for all the model parameters, in general. GetDist Python package [41] is used to analyse the obtained MCMC samples.

In the present work, we have considered variable EoS of DE in CPL form with the motivation to investigate its possible effects and deviations from our previous study [23]. We have also included neutrino mass scheme following normal hierarchy with a minimum sum of neutrino mass 0.06 eV. We have considered N_{eff} , effective number of relativistic species as a free parameter. Finally, the base parameters set of the underlying model is:

$$\{100\omega_b, \omega_{\text{cdm}}, 100\theta_s, \ln 10^{10}A_s, n_s, \tau_{\text{reio}}, w_{\text{de0}}, w_{\text{de1}}, \sum m_\nu, N_{\text{eff}}, \Gamma_\gamma\},$$

where the first six parameters pertain to the standard Λ CDM model [42].

4 Results and Discussion

The observational constraints on baseline parameters and some derived parameters of the underlying model are shown in Table 2 with four data combinations: CMB + BAO, CMB + BAO + HST, CMB + BAO + LSS and CMB + BAO + HST + LSS (joint analysis). The first six parameters are well consistent with the standard Λ CDM cosmology. With all data combinations, the mean values of w_{de0} indicate quintessence behaviour ($w_{\text{de0}} > -1$) of DE. See the one-dimensional marginalized distribution of w_{de0} in left panel of Fig. 3, where the vertical dotted line corresponds to $w_{\text{de0}} = -1$ (EoS of the DE given by cosmological constant). On the other hand, in our previous work [23] with constant EoS of DE, the mean values of w_{de0} were in the phantom region ($w_{\text{de0}} < -1$) with all data combinations. The DM-photon coupling parameter Γ_γ is approximately of the order 10^{-5} (upper 95% CL) with all data combinations under consideration (see the one-dimensional marginalized distribution of Γ_γ in the right panel of Fig. 3). These constraints on Γ_γ are similar to those obtained in our previous work [23] where a constant EoS of DE was assumed. Thus, the time-varying EoS of DE does not have any significant effect on the DM-photon coupling parameter Γ_γ .

Table 2: Constraints (68% and 95% CL) on the free parameters and some derived model parameters with four different data combinations are displayed. The parameters H_0 and $\sum m_\nu$ are measured in the units of $\text{km s}^{-1} \text{Mpc}^{-1}$ and eV, respectively. The χ^2_{\min} values of the fit are also shown in last row.

Parameter	CMB + BAO	CMB + BAO + HST	CMB + BAO + LSS	CMB + BAO + HST + LSS
$10^2 \omega_b$	$2.22^{+0.15+0.19}_{-0.08-0.22}$	$2.32^{+0.08+0.08}_{-0.03-0.12}$	$2.25^{+0.14+0.16}_{-0.06-0.21}$	$2.31^{+0.08+0.09}_{-0.03-0.13}$
ω_{cdm}	$0.121^{+0.013+0.019}_{-0.009-0.021}$	$0.131^{+0.007+0.013}_{-0.006-0.014}$	$0.121^{+0.012+0.018}_{-0.008-0.021}$	$0.127^{+0.007+0.011}_{-0.006-0.013}$
$100\theta_s$	$1.0415^{+0.0009+0.0020}_{-0.0010-0.0018}$	$1.0407^{+0.0007+0.0014}_{-0.0007-0.0013}$	$1.0414^{+0.0008+0.0021}_{-0.0010-0.0018}$	$1.0409^{+0.0007+0.0014}_{-0.0007-0.0014}$
$\ln 10^{10} A_s$	$3.095^{+0.037+0.079}_{-0.043-0.074}$	$3.102^{+0.039+0.079}_{-0.039-0.076}$	$3.115^{+0.043+0.083}_{-0.043-0.082}$	$3.112^{+0.042+0.085}_{-0.042-0.085}$
n_s	$0.974^{+0.013+0.025}_{-0.013-0.024}$	$0.975^{+0.012+0.024}_{-0.012-0.024}$	$0.976^{+0.012+0.025}_{-0.013-0.023}$	$0.977^{+0.012+0.026}_{-0.013-0.023}$
τ_{reio}	$0.080^{+0.017+0.038}_{-0.020-0.035}$	$0.080^{+0.019+0.038}_{-0.019-0.038}$	$0.092^{+0.019+0.038}_{-0.019-0.038}$	$0.092^{+0.020+0.040}_{-0.020-0.036}$
w_{de0}	$-0.76^{+0.24+0.37}_{-0.16-0.43}$	$-0.89^{+0.18+0.32}_{-0.16-0.33}$	$-0.86^{+0.24+0.38}_{-0.16-0.43}$	$-0.93^{+0.19+0.30}_{-0.14-0.33}$
w_{de1}	$-0.85^{+0.22+1.00}_{-0.62-0.68}$	$-0.62^{+0.42+0.98}_{-0.59-0.88}$	$-0.88^{+0.18+0.96}_{-0.61-0.66}$	$-0.80^{+0.26+0.92}_{-0.65-0.72}$
$\sum m_\nu [95\% \text{ CL}]$	< 0.39	< 0.52	< 0.86	< 0.89
N_{eff}	$3.29^{+0.39+0.77}_{-0.39-0.81}$	$3.60^{+0.32+0.65}_{-0.32-0.61}$	$3.40^{+0.43+0.85}_{-0.43-0.89}$	$3.62^{+0.34+0.68}_{-0.34-0.65}$
$\Gamma_\gamma [95\% \text{ CL}]$	$< 2.7 \times 10^{-5}$	$< 5.1 \times 10^{-6}$	$< 2.2 \times 10^{-5}$	$< 7.7 \times 10^{-6}$
Ω_m	$0.320^{+0.023+0.043}_{-0.023-0.045}$	$0.302^{+0.016+0.031}_{-0.016-0.030}$	$0.308^{+0.024+0.043}_{-0.021-0.046}$	$0.299^{+0.016+0.031}_{-0.016-0.031}$
H_0	$67.4^{+3.9+8.0}_{-3.9-8.0}$	$72.2^{+1.6+3.2}_{-1.6-3.0}$	$69.8^{+4.1+8.0}_{-4.1-8.0}$	$72.5^{+1.5+2.9}_{-1.5-2.9}$
σ_8	$0.799^{+0.020+0.052}_{-0.026-0.045}$	$0.816^{+0.022+0.042}_{-0.020-0.047}$	$0.761^{+0.017+0.040}_{-0.021-0.037}$	$0.767^{+0.014+0.031}_{-0.016-0.028}$
r_{drag}	$146.4^{+4.8+13}_{-7.9-11}$	$140.3^{+2.9+7.5}_{-4.1-6.1}$	$144.8^{+4.5+14.0}_{-7.5-11.0}$	$141.0^{+2.8+7.6}_{-4.3-6.3}$
$\chi^2_{\min}/2$	5640.95	5641.80	5648.78	5649.02

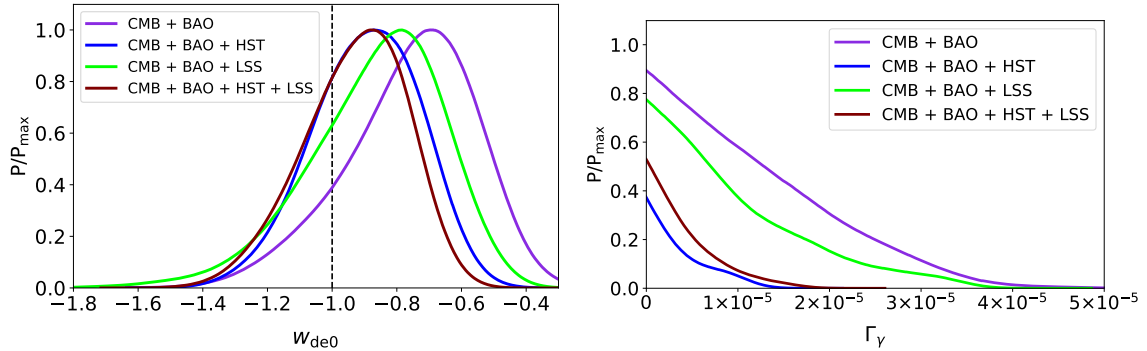


Figure 3: One-dimensional marginalized distributions of w_{de0} (left panel) and Γ_γ (right panel).

Next, we discuss the impact of the time-varying EoS of DE on H_0 and σ_8 in the context of the well-known tensions on these parameters investigated in several studies [43, 44, 45, 46, 47, 48, 49, 50, 51, 52, 53, 54, 55, 56]. In Fig. 4, we have shown the parametric space of $H_0 - \sigma_8$ obtained in our previous study (left panel) in contrast with the present study (right panel), where the horizontal yellow band shows local value $H_0 = 73.24 \pm 1.74 \text{ km s}^{-1} \text{Mpc}^{-1}$, reported by Riess *et al.* [34] whereas the vertical light red band represents the Planck-SZ measurement: $\sigma_8 = 0.75 \pm 0.03$ [35]. We notice a clear deviations in the probability regions of the H_0 and σ_8 parameters resulting due to the inception of time-varying DE in the present study. These deviations are useful to alleviate the H_0 and σ_8 tensions, as discussed in the following.

From Table 2, one can see that with the base data set: CMB + BAO, $H_0 = 67.4 \pm 3.9 \text{ Kms}^{-1} \text{Mpc}^{-1}$ at 68% CL, consistent with the Planck measurement [29]. However, with the inclusion of HST and LSS data to the base data, we have $H_0 = 72.2 \pm 1.6 \text{ Kms}^{-1} \text{Mpc}^{-1}$ and $H_0 = 69.8 \pm 4.1 \text{ Kms}^{-1} \text{Mpc}^{-1}$, both at 68% CL, respectively. In the joint analysis, we obtain $H_0 = 72.5 \pm 1.5 \text{ Kms}^{-1} \text{Mpc}^{-1}$ at 68% CL. Thus addition of HST and LSS data yields larger values of H_0 , in line with the local value $H_0 = 73.24 \pm 1.74 \text{ Kms}^{-1} \text{Mpc}^{-1}$ as

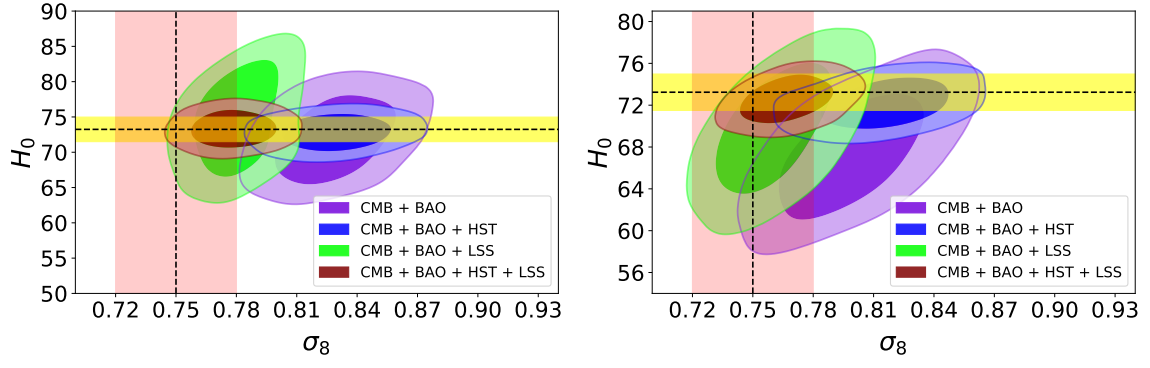


Figure 4: 68% and 95% confidence contours for H_0 and σ_8 in our previous study [23] (left panel) and in present study (right panel). In both panels, the horizontal yellow band shows local value $H_0 = 73.24 \pm 1.74 \text{ km s}^{-1} \text{ Mpc}^{-1}$, reported by Riess *et al.* [34] whereas the vertical light red band represents the Planck-SZ measurement: $\sigma_8 = 0.75 \pm 0.03$ [35].

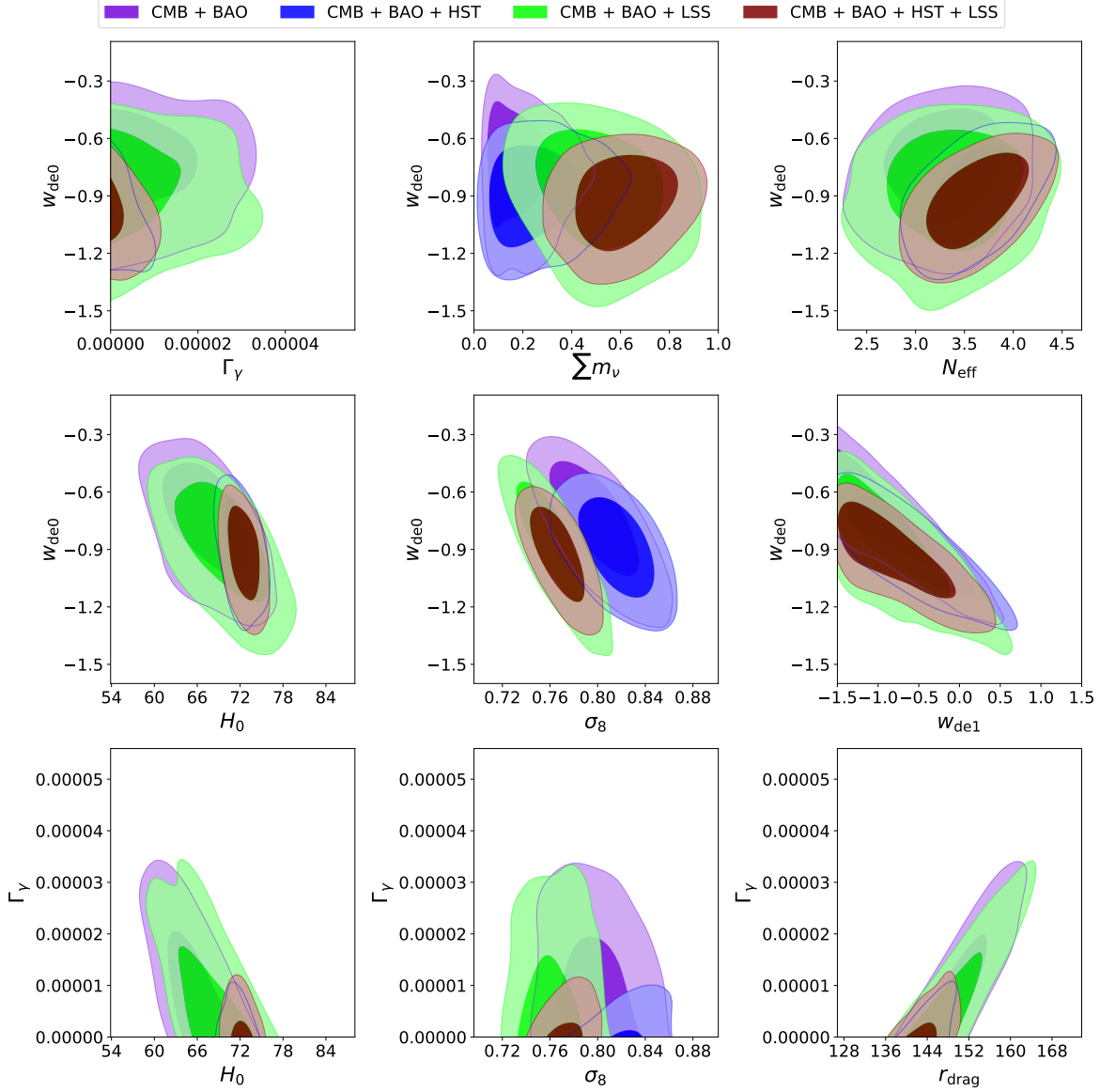


Figure 5: 68% and 95% confidence contours for some selected model parameters.

reported by Riess *et al.* [34]. In the present analysis, we have obtained lower mean values on H_0 in all the four cases as compared to our previous work [23] but still consistent with the local measurement at 68% CL (see Fig. 4).

With regard to σ_8 tension, one can note from the Table 2 that we have obtained lower values with $\sigma_8 = 0.799^{+0.020}_{-0.026}$, $\sigma_8 = 0.761^{+0.017}_{-0.021}$ and $\sigma_8 = 0.767^{+0.014}_{-0.016}$, all at 68% CL from CMB + BAO, CMB + BAO + LSS and the joint analysis, respectively. These values are in good agreement with the direct measurements like galaxy cluster count, weak gravitational lensing and Sunyaev-Zeldovich cluster abundance measurements, etc. However, with the case CMB + BAO + HST, we have $\sigma_8 = 0.816^{+0.022}_{-0.020}$ at 68% CL, favouring Planck CMB measurement. We observe that variable EoS of DE provides slightly lower values of σ_8 with all data combinations as compared to our previous results in [23]. In particular, a significant change is observed with the data combinations: CMB + BAO and CMB + BAO + LSS. One may see the consistency of the range of σ_8 values in the present study, with the Planck-SZ measurement $\sigma_8 = 0.75 \pm 0.03$ [35] (also see the right panel of Fig. 4).

Further, one may see the correlation of present DE EoS parameter w_{de0} and DM-photon coupling parameter Γ_γ with some other model parameters in Fig. 5. In particular, we observe that w_{de0} shows a negative correlation with σ_8 and H_0 parameters with all data combinations. Thus, higher values of w_{de0} correspond to lower values of σ_8 . In general, we notice that w_{de0} and Γ_γ show correlation with all other parameters especially in case of the full data combination. Next, we have found the upper bound on the neutrino mass scale as $\sum m_\nu < 0.89$ eV at 95% CL with joint analysis: CMB + BAO + HST + LSS. We notice that the constraints on neutrino mass scale are similar to those obtained in our previous study [23], with all data combinations. Also, one can see from Fig. 5 that w_{de0} does not exhibit correlation with neutrino mass scale $\sum m_\nu$. Thus, we observe that time-varying DE does not have any significant effect on the neutrino mass scale. Next, in comparison to our previous work, here we have found significantly lower values $N_{\text{eff}} = 3.29 \pm 0.39$ and $N_{\text{eff}} = 3.40 \pm 0.40$, both at 68% CL with CMB + BAO and CMB + BAO + LSS, respectively. The constraints on N_{eff} with other two data combinations are consistent with our previous work. We have obtained constraints on r_{drag} similar to our previous work [23]. In Fig. 5, one can see a positive correlation between Γ_γ and r_{drag} . The constraints on r_{drag} are in good agreement with the recent measures in [29, 57, 58] at 68% CL.

5 Statistical Model Comparison

In this section, we perform statistical comparison of the considered model with a known well-fitted reference model (here we have chosen the Λ CDM model). For this purpose, we use classical statistical criterion, namely, the Akaike Information Criterion (AIC) [59, 60], derived from information theory and defined as

$$\text{AIC} = -2 \ln \mathcal{L}_{\text{max}} + 2\mathcal{N} = \chi^2_{\text{min}} + 2\mathcal{N},$$

where \mathcal{L}_{max} is the maximum value of the likelihood function for the model, and \mathcal{N} is the total number of estimated parameters in the model. To compare the considered model i with a reference model j , we need to determine the difference of AIC values of the two models, i.e., $\Delta\text{AIC}_{ij} = \text{AIC}_i - \text{AIC}_j$. This difference can be used to interpret the evidence in favor of the model i compared to the model j . As argued in [61], one can confidently declare that one model is better than the other if the difference of AIC values of the two models is greater than a threshold value $\Delta_{\text{threshold}}$. The thumb rule of AIC states that $\Delta_{\text{threshold}} = 5$ is the universal value of threshold irrespective of the properties of the model considered for comparison. It is clearly stated in [62] that this threshold value is the minimum required difference of AIC values of the two models to strongly claim that one model is better in comparison to the other model. Thus, an AIC difference of 5 or more favors the model with smaller AIC value. Also, a model with large number of parameters is penalized in AIC criterion.

Table 3 summarizes the difference of AIC values, i.e., ΔAIC of the considered model with respect to the standard Λ CDM model for all data combinations. We have found that ΔAIC value is greater than the threshold value for the data combinations: CMB + BAO and CMB + BAO + HST. Therefore, it can be claimed that with these two data combinations, the standard Λ CDM model is strongly favored over the model under consideration. For the other combinations: CMB + BAO + LSS and CMB + BAO + HST + LSS, we can not claim statistical evidence in favor or disfavour of either of the models on the basis of AIC difference since ΔAIC is less than the threshold value. Although, a mild statistical preference of the considered model is observed in the joint analysis: CMB + BAO + HST + LSS.

Table 3: Difference of AIC values of considered model with respect to minimal Λ CDM model with considered data combinations.

Data	Δ AIC
CMB + BAO	9.56
CMB + BAO + HST	7.36
CMB + BAO + LSS	-1.34
CMB + BAO + HST + LSS	-4.80

6 Final Remarks

In this Paper, we have investigated DM-photon coupling model with time-varying EoS of DE via CPL parametrization. We have observed significant changes due to the time-varying EoS of DE on various model parameters by comparing with our previous study [23], where a constant EoS of DE was assumed. We have found that in the DM-photon coupling scenario the mean value of $w_{\text{de}0}$ favors quintessence behavior ($w_{\text{de}0} > -1$) of DE with all data combinations (see left panel of Fig. 3). We have observed significant correlations of the DE EoS parameter $w_{\text{de}0}$ with other model parameters (see Fig. 5). Due to the decay of DM into photons, we have obtained higher values of H_0 , consistent with the local measurements, similar to our previous study. In addition, the time-varying DE leads to lower values of σ_8 in the DM-photon coupling model with all data combinations, in comparison to the results in our previous study. Thus, allowing time-varying DE in the DM-photon coupling scenario is useful to alleviate the H_0 and σ_8 tensions (see Fig. 4).

Acknowledgments

The author sincerely thanks to S. Kumar and R. C. Nunes for fruitful discussions and suggestions in improving the manuscript. The author acknowledges the Council of Scientific & Industrial Research (CSIR), Govt. of India, New Delhi, for awarding Senior Research Fellowship (File No. 09/719(0073)/2016-EMR-I).

References

- [1] G. Bertone, D. Hooper, and J. Silk, *Particle dark matter: evidence, candidates and constraints*, Phys. Rept. **405** (2005) 279 [arXiv:hep-ph/0404175].
- [2] J. L. Feng, *Dark matter candidates from particle physics and methods of detection*, Ann. Rev. Astron. Astrophys. **48** (2010) 495 [arXiv:1003.0904].
- [3] A. Ibarra, D. Tran, and C. Weniger, *Indirect searches for decaying dark matter*, Int. J. Mod. Phys. A **28** (2013) 1330040 [arXiv:1307.6434].
- [4] A. Esmaili, S. K. Kang, and P. D. Serpico, *IceCube events and decaying dark matter: hints and constraints*, J. Cosmol. Astropart. Phys. **12** (2014) 054 [arXiv:1410.5979].
- [5] J. Lesgourgues, G. M. Tavares, and M. Schmaltz, *Evidence for dark matter interactions in cosmological precision data?*, J. Cosmol. Astropart. Phys. **02** (2016) 037 [arXiv:1507.04351].
- [6] N. F. Bell, A. J. Galea, and K. Petraki, *Lifetime constraints for late dark matter decay*, Phys. Rev. D **82** (2010) 023514 [arXiv:1004.1008].
- [7] N. F. Bell, A. J. Galea, and R. R. Volkas, *A model for late dark matter decay*, Phys. Rev. D **83** (2011) 063504 [arXiv:1012.0067].
- [8] K. Enqvist *et al.*, *Decaying dark matter and the tension in σ_8* , J. Cosmol. Astropart. Phys. **09** (2015) 067 [arXiv:1505.05511].
- [9] Z. Berezhiani, A. D. Dolgov, and I. I. Tkachev, *Reconciling Planck results with low redshift astronomical measurements*, Phys. Rev. D **92** (2015) 061303 [arXiv:1505.03644].
- [10] V. Poulin, P. D. Serpico, and J. Lesgourgues, *A fresh look at linear cosmological constraints on a decaying dark matter component*, J. Cosmol. Astropart. Phys. **08** (2016) 036 [arXiv:1606.02073].

- [11] P. Ko and Y. Tang, *Light dark photon and fermionic dark radiation for the Hubble constant and the structure formation*, Phys. Lett. B **762** (2016) 462 [arXiv:1608.01083].
- [12] M. A. B. Abad *et al.*, *Interacting dark sector and precision cosmology*, J. Cosmol. Astropart. Phys. **01** (2018) 008 [arXiv:1708.09406].
- [13] S. L. Amigo *et al.*, *Cosmological constraints on decaying dark matter*, J. Cosmol. Astropart. Phys. **06** (2009) 005 [arXiv:0812.4016].
- [14] I. M. Oldengott, D. Boriero, and D. J. Schwarz; *Reionization and dark matter decay*, J. Cosmol. Astropart. Phys. **08** (2016) 054 [arXiv:1605.03928].
- [15] C. E. Aisati *et al.*, *Dark matter decay to a photon and a neutrino: the double monochromatic smoking gun scenario*, Phys. Rev. D **93** (2016) 043535 [arXiv:1510.05008].
- [16] M. Gustafsson, T. Hambye, and T. Scarna, *Effective theory of dark matter decay into monochromatic photons and its implications: constraints from associated cosmic-ray emission*, Phys. Lett. B **724** (2013) 288 [arXiv:1303.4423].
- [17] H. Yuksel and M. D. Kistler, *Circumscribing late dark matter decays model independently*, Phys. Rev. D **78** (2008) 023502 [arXiv:0711.2906].
- [18] C. Boehm *et al.*, *Interacting dark matter disguised as warm dark matter*, Phys. Rev. D **66** (2002) 083505 [arXiv:astro-ph/0112522].
- [19] J. Stadler and C. Boehm, *CMB constraints on γ -CDM interactions revisited*, J. Cosmol. Astropart. Phys. **10** (2018) 009 [arXiv:1802.06589].
- [20] R. J. Wilkinson, J. Lesgourgues, and C. Boehm, *Using the CMB angular power spectrum to study dark matter-photon interactions*, J. Cosmol. Astropart. Phys. **04** (2014) 026 [arXiv:1309.7588].
- [21] R. J. Wilkinson, C. Boehm, and J. Lesgourgues, *Constraining dark matter-neutrino interactions using the CMB and large-scale structure*, J. Cosmol. Astropart. Phys. **05** (2014) 011 [arXiv:1401.7597].
- [22] S. Kumar and R. C. Nunes, *Observational constraints on dark matter-dark energy scattering cross section*, Eur. Phys. J. C **77** (2017) 734 [arXiv:1709.02384].
- [23] S. Kumar and R. C. Nunes, and S. K. Yadav, *Cosmological bounds on dark matter-photon coupling*, Phys. Rev. D **98** (2018) 043521 [arXiv:1803.10229].
- [24] M. Chevallier and D. Polarski, *Accelerating Universes with scaling dark matter*, Int. J. Mod. Phys. D **10** (2001) 02 [arXiv:gr-qc/0009008].
- [25] E. V. Linder, *Exploring the expansion history of the Universe*, Phys. Rev. Lett. **90** (2003) 091301 [arXiv:astro-ph/0208512].
- [26] S. Kumar, *Probing the matter and dark energy sources in a viable Big Rip model of the Universe*, Mod. Phys. Lett. A **29** (2014) 1450119 [arXiv:1404.1910].
- [27] S. Kumar and L. Xu, *Observational constraints on variable equation of state parameters of dark matter and dark energy after Planck*, Phys. Lett. B **7** (2014) 737 [arXiv:1207.5582].
- [28] W. Yang and L. Xu, *Cosmological constraints on interacting dark energy with redshift-space distortion after Planck data*, Phys. Rev. D **89** (2014) 083517 [arXiv:1401.1286].
- [29] P. A. R. Ade *et al.* (Planck collaboration), *Planck 2015 results-xiii. cosmological parameters*, A & A **594** (2016) A13 [arXiv:1502.01589].
- [30] F. Beutler *et al.*, *The 6dF Galaxy survey: baryon acoustic oscillations and the local Hubble constant*, Mon. Not. Roy. Astron. Soc. **416** (2011) 3017 [arXiv:1106.3366].
- [31] A. J. Rosset *et al.*, *The clustering of the SDSS DR7 main Galaxy sample I: a 4 per cent distance measure at $z = 0.15$* , Mon. Not. Roy. Astron. Soc. **449** (2015) 835 [arXiv:1409.3242].
- [32] L. Anderson *et al.*, *The clustering of galaxies in the SDSS-III baryon oscillation spectroscopic survey: baryon acoustic oscillations in the data release 10 and 11 galaxy samples*, Mon. Not. Roy. Astron. Soc. **441** (2014) 24 [arXiv:1312.4877].

- [33] R. C. Nunes *et al.*, *New observational constraints on $f(R)$ gravity from cosmic chronometers*, J. Cosmol. Astropart. Phys. **01** (2017) 005 [arXiv:1610.07518].
- [34] A. G. Riess *et al.*, *A 2.4% determination of the local value of the Hubble constant*, Astrophys. J. **826** (2016) 56 [arXiv:1604.01424].
- [35] P. A. R. Ade *et al.* (Planck collaboration), *Planck 2013 results. XX. Cosmology from Sunyaev-Zeldovich cluster counts*, A & A **571** (2014) A20 [arXiv:1303.5080].
- [36] C. Heymans *et al.*, *CFHTLenS tomographic weak lensing cosmological parameter constraints: mitigating the impact of intrinsic galaxy alignments*, Mon. Not. Roy. Astron. Soc. **432** (2013) 2433 [arXiv:1303.1808].
- [37] F. Köhlinger *et al.*, *KiDS-450: The tomographic weak lensing power spectrum and constraints on cosmological parameters*, Mon. Not. Roy. Astron. Soc. **471** (2017) 4412 [arXiv:1706.02892].
- [38] D. Blas, J. Lesgourgues, and T. Tram, *The cosmic linear anisotropy solving system (CLASS) II: approximation schemes*, J. Cosmol. Astropart. Phys. **07** (2011) 034 [arXiv:1104.2933].
- [39] B. Audren *et al.*, *Conservative constraints on early cosmology with MONTE PYTHON*, J. Cosmol. Astropart. Phys. **02** (2013) 001 [arXiv:1210.7183].
- [40] A. Gelman and D. B. Rubin, *Inference from iterative simulation using multiple sequences*, Statist. Sci. **7** (1992) 457.
- [41] <https://github.com/cmbant/getdist>
- [42] P. A. R. Ade *et al.* (Planck collaboration), *Planck 2013 results. XVI. Cosmological parameters*, A & A **571** (2014) A16 [arXiv:1303.5076].
- [43] E. Di Valentino *et al.*, *Reducing the H_0 and σ_8 tensions with dark matter-neutrino interactions*, Phys. Rev. D **97** (2018) 043513 [arXiv:1710.02559].
- [44] S. Pan *et al.*, *Observational constraints on sign-changeable interaction models and alleviation of the H_0 tension*, [arXiv:1903.10969v1].
- [45] W. Yang *et al.*, *Tale of stable interacting dark energy, observational signatures, and the H_0 tension*, J. Cosmol. Astropart. Phys. **09** (2018) 019 [arXiv:1805.08252].
- [46] S. Pan, W. Yang, and A. Paliathanasis, *Imprints of an extended Chevallier-Polarski-Linder parametrization on the large scales*, [arXiv:1902.07108v1].
- [47] M. Du *et al.*, *Future constraints on dynamical dark-energy using Gravitational-Wave standard sirens*, [arXiv:1812.01440].
- [48] W. Yang *et al.*, *Effects of neutrino mass hierarchies on dynamical dark energy models*, Phys. Rev. D **95** (2017) 103522 [arXiv:1703.02556].
- [49] S. Kumar and R. C. Nunes, *Probing the interaction between dark matter and dark energy in the presence of massive neutrinos*, Phys. Rev. D **94** (2016) 123511 [arXiv:1702.02143].
- [50] S. Kumar and R. C. Nunes, *Echo of interactions in the dark sector*, Phys. Rev. D **96** (2017) 103511 [arXiv:1702.02143].
- [51] S. Kumar and R. C. Nunes, and S. K. Yadav, *Dark sector interaction: a remedy of the tensions between CMB and LSS data*, Eur. Phys. J. C **79** (2019) 576 [arXiv:1903.04865].
- [52] E. Di Valentino, A. Melchiorri, and O. Mena, *Can interacting dark energy solve the H_0 tension ?*, Phys. Rev. D **96** (2017) 043503 [arXiv:1704.08342].
- [53] V. Poulin *et al.*, *The implications of an extended dark energy cosmology with massive neutrinos for cosmological tensions*, Phys. Rev. D **97** (2018) 123504 [arXiv:1803.02474].
- [54] Rafael C. Nunes, *Structure formation in $f(T)$ gravity and a solution for H_0 tension*, J. Cosmol. Astropart. Phys. **05** (2018) 052 [arXiv:1802.02281].
- [55] S. M. Feeney *et al.*, *Prospects for resolving the Hubble constant tension with standard sirens*, Phys. Rev. Lett. **122** (2019) 061105 [arXiv:1802.03404].

- [56] M. Benetti, L. L. Graef, and J. S. Alcaniz, *The H_0 and σ_8 tensions and the scale invariant spectrum*, J. Cosmol. Astropart. Phys. **066** (2018) 07 [arXiv:1712.00677].
- [57] A. Heavens, R. Jimenez, and L. Verde, *Standard rulers, candles, and clocks from the low-redshift Universe*, Phys. Rev. Lett. **113** (2014) 241302 [arXiv:1409.6217].
- [58] L. Verde *et al.*, *The length of the low-redshift standard ruler*, Mon. Not. Roy. Astron. Soc. **467** (2017) 731 [arXiv:1607.05297].
- [59] H. Akaike, *A new look at the statistical model identification*, IEEE Trans. Autom. Control **19**, 716, 1974.
- [60] K. P. Burnham and D. R. Anderson, *Model selection and multimodel inference*, (Springer, New York, 2002).
- [61] M. Y. J. Tan and R. Biswas, *The reliability of the Akaike information criterion method in cosmological model selection*, Mon. Not. Roy. Astron. Soc. **4**, 419, 2012.
- [62] A. R. Liddle, *Information criteria for astrophysical model selection*, Mon. Not. Roy. Astron. Soc. **1**, 377, 2007 arXiv:astro-ph/0701113.